Shunt and Rogowski coil measurements on ASDEX Upgrade in support of DEMO detachment control

L. Giannone[a], S.El Shawish[b], A.Herrmann[a], A.Kallenbach[a], K.H.Schuhbeck[a], G.Vayakis[c], C.Watts[c], I. Zammuto[a], ASDEX Upgrade team[d]

[a]*Max Planck Institute for Plasma Physics, 85748 Garching, Germany*
[b]*Jožef Stefan Institute, Jamova 39, SI-1000 Ljubljana, Slovenia*
[c]*ITER Organization, Route de Vinon, F-13115 St Paul lez Durance, France*
[d]*see the author list of H. Meyer et al. 2019 Nucl. Fusion 59 112014*

Abstract

Detachment control in DEMO is a fundamental requirement to prevent damage to the plasma facing components. Thermo-currents flowing through the plasma facing components of the divertor cassette are driven by the thermoelectric voltage generated by the plasma temperature difference between the inner and outer target plates. Shunt and Rogowski coil measurements to measure thermo-currents for detachment control on ITER are planned. Thermo-current measurements on ASDEX Upgrade have been carried out in support of establishing designs considered suitable to measure thermo-currents in DEMO.

Keywords: DEMO divertor, Thermo-current, Detachment control, Shunt resistance, Rogowski coil, Plasma facing component

1. Introduction

In present tokamaks, the heat load on to the target plates of the divertor must be controlled to avoid damage. A thermoelectric voltage is generated by the plasma temperature difference between the inner and outer target plates of the divertor cassette. This voltage drives the halo current that flows in the scrape off layer of a tokamak [1]. By measuring the thermo-current flowing to the target plate (indirectly measured as a voltage over a

Email address: Louis.Giannone@ipp.mpg.de (L. Giannone)

shunt) and using nitrogen gas puffing feedback control of this tile current, plasma detachment and a decrease of the heat load to the plasma facing components in the divertor can be achieved [2, 3]. Therefore, a means for making such thermo-current measurements in DEMO will also be required.

The divertor thermo-current has been estimated using an established numerical model (Eq. 1 from [1]) and realistic parameters from ASDEX Upgrade (where the measured divertor tile current has been reproduced by the model), ITER and DEMO. The electrical current density is driven by the difference of the outer and inner divertor electron temperature at the sheath entrance, which have been set to 5 eV and 1 eV, respectively. Since the product of the average scrape-off layer resistivity and the connection length stays about the same for the 3 devices, the total current scales about linearly with the divertor circumference. Assuming a scrape-off layer power of 3 MW in AUG and 30 MW in ITER and DEMO (accounting for radiation losses in the scrape-off layer), and a midplane power e-folding width of 2 mm and a scrape-off layer Z_{eff}=2 for all 3 devices, total thermo-currents of 2.1, 6.8 and 6.9 kA are obtained for AUG, ITER and DEMO, respectively. For the 2 latter devices, these are upper bounds, since target protection may require a lower T_e in the outer divertor. The thermo-current in DEMO with 48 cassette modules (assuming the 16 toroidal field coil machine) is therefore estimated to have a steady state value for an attached plasma of about 150 A for each cassette. The thermo-current in ITER with 54 cassette modules (assuming the 18 toroidal field coil machine) is therefore estimated to have a steady state value for an attached plasma of about 130 A for each cassette.

A split divertor design to facilitate the thermo-current measurements by the insertion of a shunt resistor between the two divertor cassette parts was not considered feasible, owing to remote handling issues and the forces generated by the current in the water-cooling pipes in the event of a disruption. In Section 2, the designs for ITER shunts and Rogowksi coils for measuring divertor cassette currents are summarised. In Section 3, previous work on DEMO shunts with plasma facing components isolated from the divertor cassette is reviewed. Difficulties arise when using Rogowski coils around the divertor cassette as an alternative method for measurement of the divertor thermo-currents. Measurements using a Rogowski coil mounted on the heat shield support in ASDEX Upgrade are used to illustrate these difficulties in Section 4. The feasibility of using the divertor cassette in DEMO as a shunt to measure thermo-currents is discussed in section 5. A proof of

principle experiment was carried out on ASDEX Upgrade by introducing a 50 $\mu\Omega$ shunt to produce signal levels expected when using the DEMO divertor cassette as a shunt.

2. ITER shunts and Rogowski coils

On ITER, the resistance of the divertor cassette has been modelled [4], giving the profile as shown in Fig. 1. The analysis is static, i.e.) the value of divertor resistance is valid for very slow EM transients (typically for characteristic times greater than 0.1, 0.2 s). This simulation indicates that the total resistance of the divertor is 46.5 $\mu\Omega$. The resistance between any two shunt test points on the divertor cassette is typically 6 - 7 $\mu\Omega$, giving a sensitivity of 6 mV/kA. Once the actual cassette assemblies are available, the shunts will be directly calibrated by applying a voltage drop along the cassette body. For the estimated thermo-current in ITER (130 A), a shunt voltage measurement of about 0.8 mV is predicted.

In Fig. 2, the placement of Rogowski coils, planned to measure currents flowing in the divertor cassette of ITER, are shown [5, 6]. These coils are designed to measure the estimated 120 kA halo current flowing through the cassette following a disruption. The divertor Rogowski coil consists of two winding layers of mineral insulated cable, wound forwards and then in the reverse direction with the same pitch. A prototype is shown in Fig. 3. Preliminary designs have a total of 6500 turns with a cross-section of 150 mm^2 over a length of up to 3 m. With an integration time of 10 ms, a sensitivity of 40.8 mV/kA could be achieved. A Rogowski coil on the DEMO divertor cassette with this sensitivity would then deliver a signal of 6.1 mV for the estimated 150 A of divertor thermo-current per cassette.

It has been recognised that the vacuum vessel attachment of the divertor cassette provides an alternative path for the thermo-current (see next section for details). Preliminary calculations suggest that 33% of the current would flow through the divertor cassette and 66% would flow through the vacuum vessel wall. A Rogowskii coil wound around the cassette with approximately 50 A thermo-current therefore would only have an expected a signal level of 2.0 mV.

3. DEMO shunts

Shown in Fig. 4 is a schematic diagram of a design for shunts with isolated plasma facing components to measure thermo-currents on DEMO.

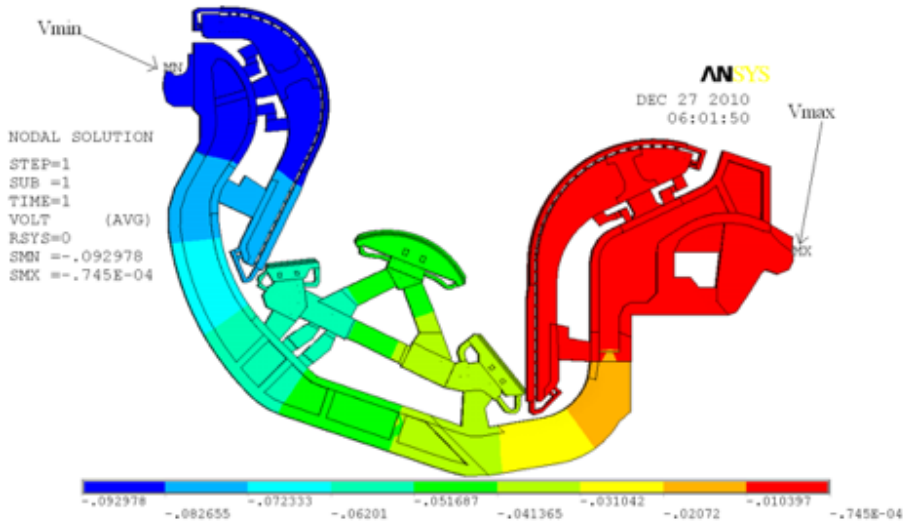

Figure 1: *Modelling of voltage drop along the ITER divertor half cassette for 1kA current [4]*

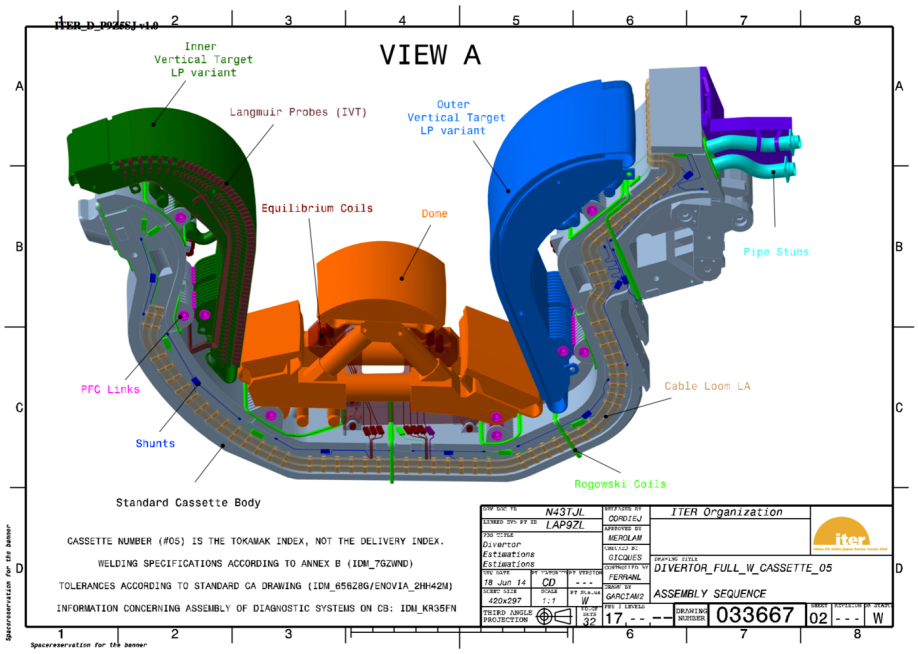

Figure 2: *Shunts and Rogowski coils planned for the ITER divertor cassette [5]*

Figure 3: *Rogowski coil prototype for the ITER divertor cassette*

The isolation of the plasma facing components is achieved using an alumina coating on the leg supports [7].

The cassette-to-vacuum vessel fixation system works as an interface between the divertor system and vacuum vessel. It shall withstand all loads due to electromagnetic events, such as disruptions or the discharge of the magnet system and it shall ensure electrical connection between the divertor and the vessel. In addition, the outboard fixation system is designed with sufficient flexibility to accommodate differential thermal expansion of the vacuum vessel and cassette body [8].

The resistance of the DEMO divertor cassette is estimated to be 22 $\mu\Omega$. The effective resistance of the vacuum vessel sector between the supporting regions of 3 divertor cassettes is estimated to be 3.75 $\mu\Omega$. This indicates that with three divertor cassettes in parallel with a resistance of 7.3 $\mu\Omega$, roughly only a third of the thermo-current will flow through the divertor cassettes and two thirds through the vacuum vessel wall, assuming ideal conduction of the cassette fixation system.

Mechanical, thermal and electrical analyses have been performed in order to identify the number of shunts, their maximum resistances and their optimal locations in the isolated-target design model of the DEMO divertor [9]. The analyses have adopted the recent DEMO baseline 2017 divertor model [8, 10, 11] which by design precludes large pipe bending. Steady-state electrical analysis assumed realistic extreme loading conditions during a disruption. During the current quench phase of a plasma disruption the plasma current decay induces currents in the passive structures in the vacuum vessel and the plasma may move vertically. If the plasma vertical control is lost and the thermal quench occurs during plasma vertical movement the event is known as a vertical disruption event [12]. In this case, the induced halo currents through the divertor can be significantly larger than the thermo-current itself.

Based on DEMO plasma disruption simulations for a moderately slow current quench time of 400 ms carried out with an evolutionary equilibrium code, the fraction of the total halo current entering different in-vessel components has been calculated [13]. The most extreme loading conditions of a vertical disruption event type IV slow down case are assumed with 30 kA and 89 kA halo currents flowing on inner and outer PFC targets, respectively. In particular, the number of shunts, their maximum resistances and optimal locations are proposed from the requirement that the temperature of the water-cooling pipes does not exceed the water boiling temperature

and that all the pipes retain their structural integrity during the disruption. The results of the analysis suggest safe operation is possible with four shunts of 600 $\mu\Omega$ that protect the isolated cooling water pipes during the disruption event and provide a 64 mV signal for the 150 A divertor thermo-current measurement.

A pipe integrity assessment in a 2D parameter space of shunt resistance and cooling pipe contact resistance to the divertor cassette for the applied 30/89 kA current has also been carried out [14]. It is estimated that a design with cooling pipe in electrical contact with the divertor cassette and a 1 mΩ shunt would give a 10 mV signal across the inner and outer divertor.

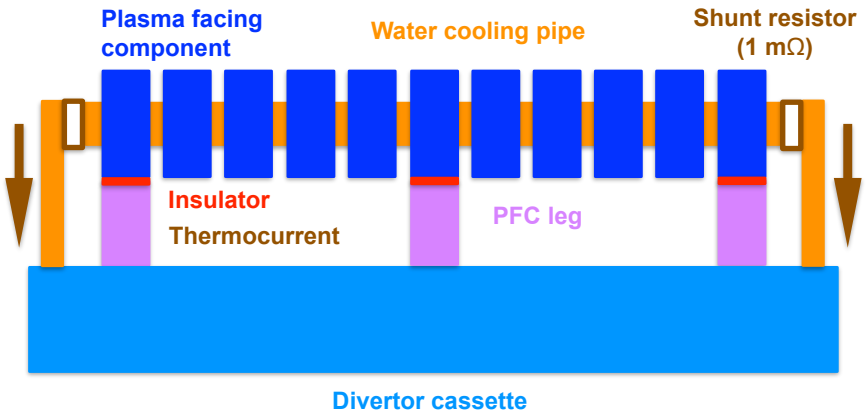

Figure 4: *Schematic diagram of a design for shunts with isolated plasma facing component legs to measure thermo-current on DEMO. The inner and outer divertor target plate each have two shunts, one on the entry water cooling pipe and one on the exit water cooling pipe.*

4. ASDEX Upgrade Rogowski coil

The quality of compensation of stray fields from the toroidal and poloidal field coil currents and the plasma current will determine whether thermo-current measurements using a Rogowski coil are good enough for feedback control. The ability to compensate these stray fields on an in-vessel Rogowski coil measurement, in this case for the current flowing in the heat shield support structure in ASDEX Upgrade, was tested. In Fig. 5, Rogowski coil measurements for the current flowing in the heat shield support structure during a vacuum discharge with poloidal and toroidal fields and

without plasma are shown (blue). The signal corrected for pickup from the currents flowing in the poloidal and toroidal fields is also shown (red). The sensitivity of this Rogowski coil is 33 mV/kA. The signal was compensated to within ±30 A. In Fig. 6, Rogowski coil measurements for the current flowing in the heat shield structure during a plasma discharge and the poloidal and toroidal field coil currents are shown (blue). The signal corrected for pickup from the currents flowing in the poloidal and toroidal field coils and in the plasma is also shown (red). Further effort is needed to produce a signal adequate for use as input to a control system for detachment control.

For DEMO, the issues of the DC performance of the Rogowski measurements as well as long term drifts of the electronic integrators will also need to be considered. A linear extrapolation of tests of the Rogowski coil on W7-X would lead to a drift of around 70 A for a pulse length of 1800 s [15]. A detailed study of the source of errors in the Rogowski coil for plasma current measurements on ITER (effect of the joints and disturbances due to external sources of field, deviations from ideal geometry, toroidal field variations, calibration, noise and integration drift) has been published [16].

It should be noted that a Rogowski coil around the DEMO divertor cassette will have to cope with a much greater neutron flux than the coils in ITER. In situ measurements of the differential voltage between the ends of two magnetic coils wound with mineral-insulated cable have been carried out at the JMTR fission reactor [17]. A voltage in the range of several μV was measured. This is higher than that which can be tolerated for ITER long pulse operation. The radiation induced voltages were attributed to transmutation of impurities in the copper wire.

Using EUROFER97 in a DEMO water-cooled divertor cassette, imposes a lower limit of the operating temperature to preserve ductility under irradiation. It has been shown that the fracture toughness transition temperature of EUROFER97 at 6 dpa (the expected maximum dose of cassette body after 2 fusion power years) is about 180°C taking the embrittlement due to helium production into account [18]. Preliminary studies show that the DEMO cassette will have temperatures up to 350°C in the region where the divertor Rogowski coil will be located [19, 20]. A robust design of a Rogowski coil around the divertor cassette of DEMO to survive the challenges faced by materials inside the vacuum vessel will require a major investment of engineering resources.

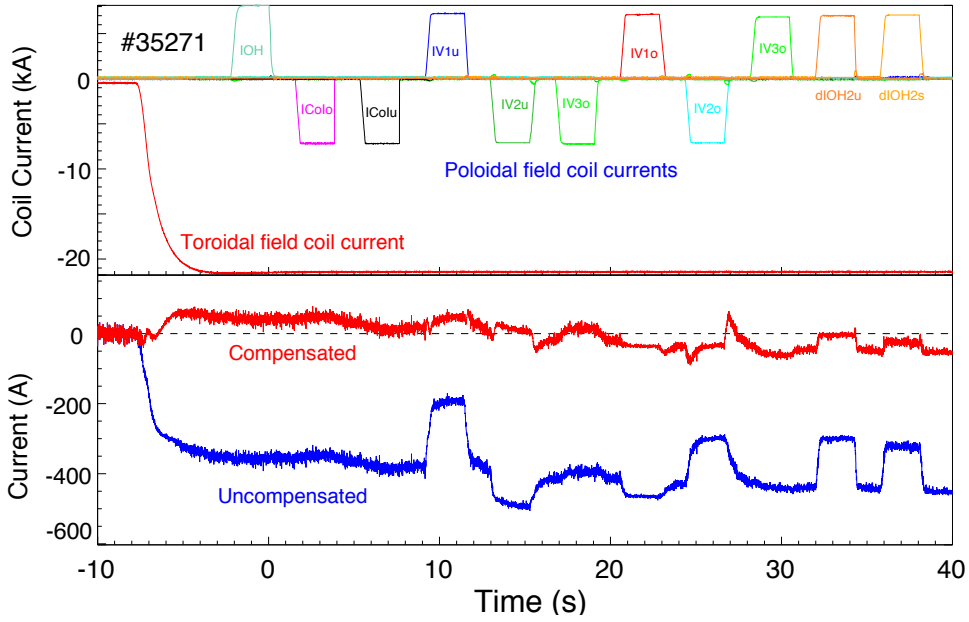

Figure 5: *Poloidal and toroidal field coil currents induce stray field pick-up in Rogowski coil measurements. The uncompensated (blue) and compensated (red) signals for current flowing in the heat shield support structure of ASDEX Upgrade in a vacuum discharge are shown.*

5. ASDEX Upgrade shunts

An alternative solution for thermo-current measurements in DEMO that does not require the isolation of the plasma facing components and divertor cassette is explored in this section. Scrape-off layer (SOL) and halo currents are measured in AUG with shunts mounted between tiles (located on the inner wall, the upper and lower divertors) and their mechanical support. The shunt consists of a hollow screw, whose cavity contains a rod of copper in contact with the tile on one side and electrically isolated along its length. The voltage drop along the stainless steel or manganin screw is measured by means of electrical contacts at its top (copper rod) and at the fastening nut at its bottom [21]. A shunt connected to a plasma facing tile normally has a resistance of 2 $m\Omega$ and measures 15 A. By reducing the shunt resistance to 50 $\mu\Omega$, the expected signal level would be 0.75 mV. For data acquisition with sufficient bit resolution, this signal is pre-conditioned by an isolation amplifier with a gain of 100 and a bandwidth of 100 kHz (Analog Devices, AD215).

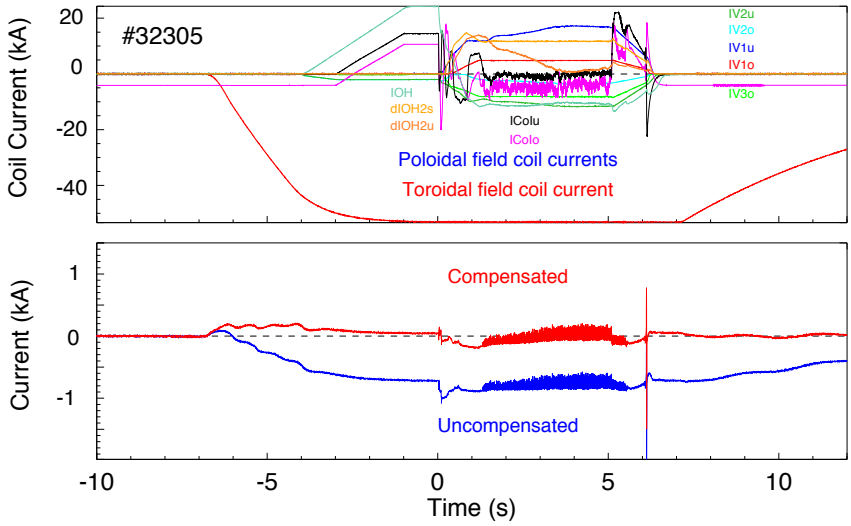

Figure 6: *Plasma current and the poloidal and toroidal field coil currents induce stray field pick-up in Rogowski coil measurements. The uncompensated (blue) and compensated (red) signals for current flowing in the heat shield support structure of ASDEX Upgrade in a plasma discharge are shown.*

Proof of principle measurements to demonstrate the feasibility of using the DEMO divertor cassette as a shunt were carried out on ASDEX Upgrade. Shown in Fig. 7 is an overview of a plasma discharge with small edge localized modes (ELM's). In Fig. 8 , the current measurements by 50 $\mu\Omega$ (10DUAu) and 2 $m\Omega$ (14DUAu) shunts with their respective smoothed control signals (Tdiv2 for the 50 $\mu\Omega$ and Tdiv for the 2 $m\Omega$ shunt) for a plasma discharge with small ELM's) is shown.

Shown in Fig. 9 is an overview of a plasma discharge with large ELM's. In Fig. 10, the current measurements by the 50 $\mu\Omega$ (10DUAu) and 2 $m\Omega$ (14DUAu) shunts with their respective smoothed control signals (Tdiv2 for the 50 $\mu\Omega$ and Tdiv for the 2 $m\Omega$ shunt) for a plasma discharge with large ELM's is shown. Looking into the shunt measurements with higher time resolution, it can be seen in Fig. 10 that oscillations in the current measurement by the 50 $\mu\Omega$ (10DUAu) shunt dominate the ELM spikes seen clearly in the current measurement by the 2 $m\Omega$ (14DUAu) shunt. These oscillations, with a typical frequency of 600 Hz, are interpreted as floating potential fluctuations on the tile surface and their visibility becomes only apparent when the signal level generated by the thermo-current is sufficiently small.

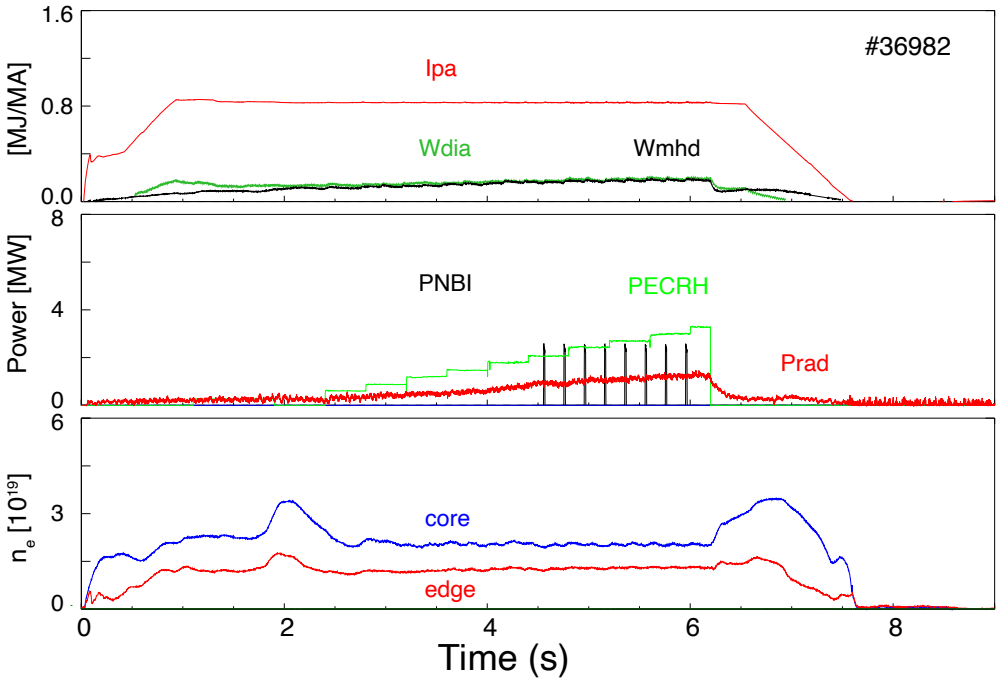

Figure 7: *Overview of plasma discharge with small ELM's in ASDEX Upgrade. The upper time traces show the plasma current (Ipa), diamagnetic energy (Wdia) and energy calculated from the magnetic equilibrium (Wmhd). The middle time traces show the radiated power (Prad) and deposited power by neutral beam injection (PNBI) and electron cyclotron heating (PECRH). The lower time traces show the line integrated density of a central (core) and edge chord (edge).*

Viewing shunt currents in Fig. 11, with higher time resolution in a subsequent discharge with lower ELM frequency, one observes in addition that oscillations in the 50 $\mu\Omega$ (10DUAu) shunt measurement vary in frequency after the ELM spikes. These changes in oscillation frequency increase the confidence that the measurements have a physical cause rather than simply being generated by the isolation amplifier in response to the ELM spikes or other external sources.

From these measurements one can conclude that limiting the heat flux to the plasma facing components in DEMO will require that plasma discharges be in a small ELM regime. In this case, the results of Fig. 12 indicate that thermo-current measurements with a signal level of 0.75 mV with suitable pre-conditioning by an isolation amplifier are feasible. This signal level will approximately be maintained in DEMO as the expected factor of 3 smaller

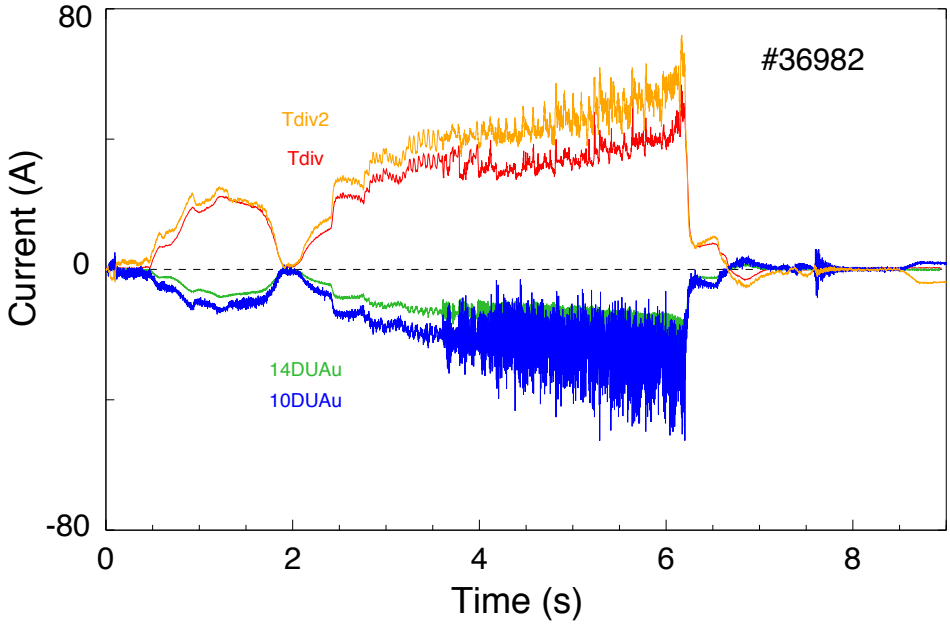

Figure 8: *Current measurements by 50 μΩ (10DUAu) and 2 mΩ (14DUAu) shunts with their respective smoothed control signals (Tdiv2 for the 50 μΩ and Tdiv for the 2 mΩ shunt) for a plasma discharge in ASDEX Upgrade with small ELM's*

shunt resistance of the divertor cassette will be compensated by an expected factor of 3 larger thermo-current (50 A) flowing through the divertor cassette. The increase in current in DEMO can also be understood in terms of a scaling of geometry between DEMO and ASDEX Upgrade. The ratio of major radii in DEMO and ASDEX Upgrade (7.5/1.65) multiplied by the ratio of the toroidal extent of a cassette in DEMO and a tile in ASDEX Upgrade (128/48) would gives a factor of 12 scaling up of expected thermo-current for DEMO. It should be noted that the extent to which signal noise will be enhanced with cables connected to connection points as in ITER or DEMO cannot be estimated from these proof of principle experiments.

6. Conclusions

Heat load control of plasma facing components in the divertor of tokamaks using shunt measurements of the thermo-current flowing between the inner and outer divertor as the feedback control parameter and impurity gas puffing to reach the set level is a well established technique. Shunt

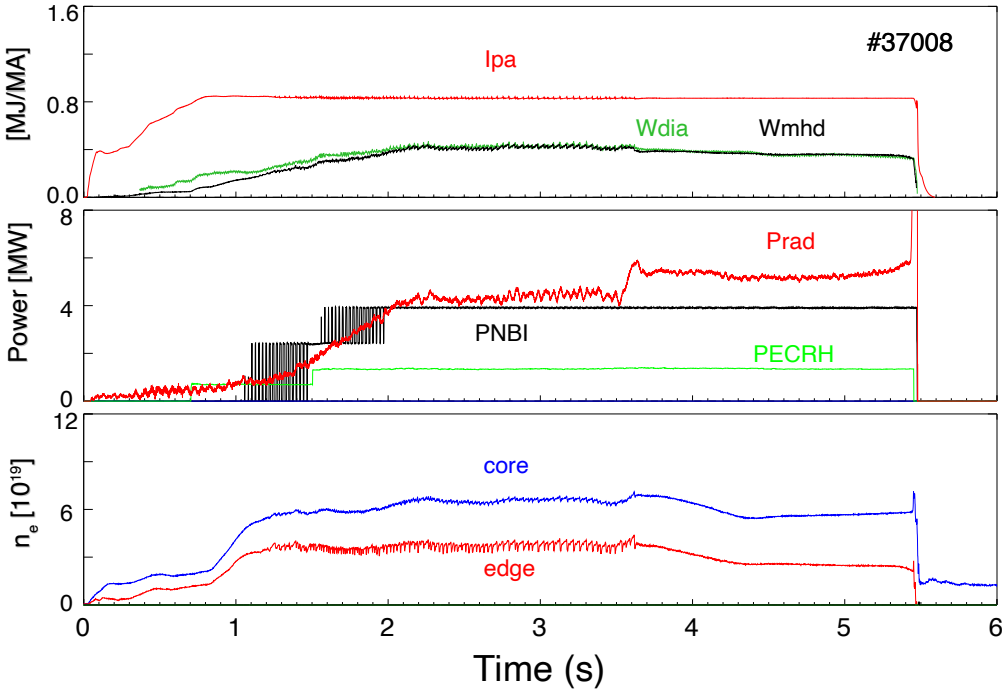

Figure 9: *Overview of plasma discharge with large ELM's in ASDEX Upgrade. The upper time traces show the plasma current (Ipa), diamagnetic energy (Wdia) and energy calculated from the magnetic equilibrium (Wmhd). The middle time traces show the radiated power (Prad) and deposited power by neutral beam injection (PNBI) and electron cyclotron heating (PECRH). The lower time traces show the line integrated density of a central (core) and edge chord (edge).*

and Rogowski coil measurements to measure thermo-currents for detachment control on ITER are planned. Experiments in ASDEX Upgrade have been carried out in support of the development of designs to carry out these measurements in DEMO.

Measurements using a Rogowski coil mounted on the heat shield support were used to illustrate the difficulties of stray field compensation of poloidal and toroidal field coil currents. The feasibility of using the divertor cassette as a shunt to measure thermo-currents was examined in proof of principle experiments. A 50 $\mu\Omega$ shunt was introduced to produce signal levels expected on DEMO when using the divertor cassette as a shunt. The results indicate that thermo-current measurements with a signal level of 0.75 mV with suitable pre-conditioning by an isolation amplifier are feasible provided that the plasma discharges are in a small ELM regime. This limitation is

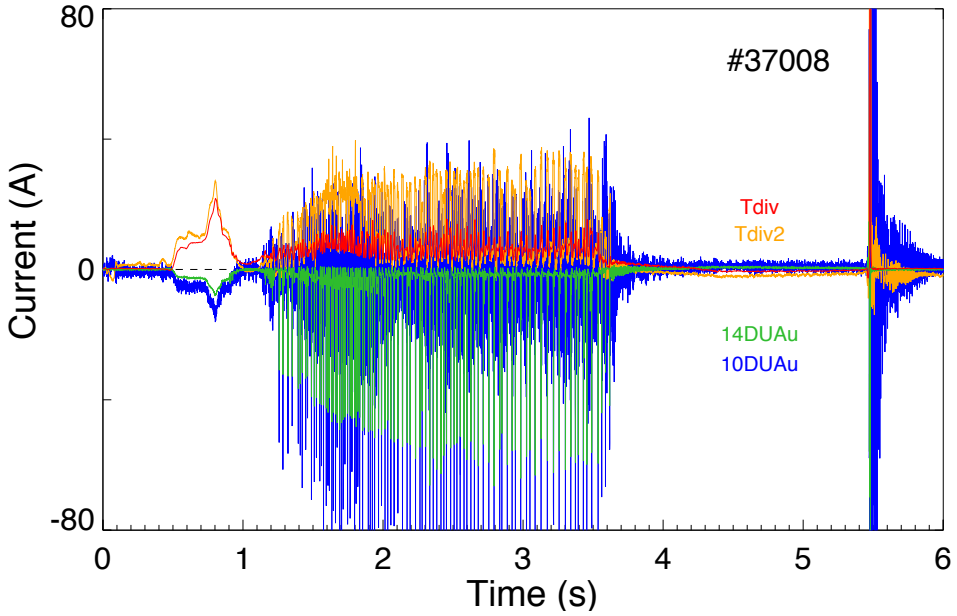

Figure 10: *Current measurements by 50 μΩ (10DUAu) and 2 mΩ (14DUAu) shunts with their respective smoothed control signals (Tdiv2 for the 50 μΩ and Tdiv for the 2 mΩ shunt) for a plasma discharge in ASDEX Upgrade with large ELM's.*

not significant as heat flux limits to the plasma facing components in DEMO require that plasma discharges be in a small ELM regime.

An isolated plasma facing component design with four 1 mΩ shunts and a cooling water pipe electrically connected to the divertor cassette is an alternative design and would produce a signal level of 10 mV.

Acknowledgements

The author would like to thank the in-vessel team for their vital contribution of mounting the shunt resistors and A. Wöls for the isolation amplifier support. The work leading to this article was funded by the European Atomic Energy Community and is subject to the provisions of the European Fusion Development Agreement. This work has been carried out within the framework of the EUROfusion Consortium and has received funding from the Euratom research and training programme 2014–2018 and 2019–2020 under grant agreement No 633053. The views and opinions expressed herein do not necessarily reflect those of the European Commission or the ITER Organization.

References

[1] A. Kallenbach, A. Carlson, G. Pautasso, et al., Electric currents in the scrape-off layer in ASDEX Upgrade, J. Nucl. Mater. 639 (2001) 290, doi:10.1016/S0022-3115(00)00445-1

[2] A. Kallenbach, M. Bernert, M. Buerskens, et al., Partial detachment of high power discharges in ASDEX Upgrade, Nucl. Fusion 55 (2015) 050326, doi:10.1088/0029-5515/55/5/053026

[3] A. Kallenbach, M. Bernert, T. Eich, et al., Optimized tokamak power exhaust with double radiative feedback in ASDEX Upgrade, Nucl. Fusion 52 (2012) 122003, doi:10.1088/0029-5515/52/12/122003

[4] M. Rocella, L.T.Calculi, Evaluation of Ohmic resistance of divertor, ITER Report ITER D 3ZZEUH (2010).

[5] C. Watts, Halo Current Rogowski Coil Reference Design, ITER Report, ITER D QE7X4N (2015).

[6] G. Chitarin, E. Alessi, M. Cavinato, et al., Design study of the ITER magnetic diagnostic: in-vessel pick-up coils, blanket halo sensors and divertor halo sensors, numerical model of halo currents, EFDA Report, EFDA 05-1347 D2.2 (2008).

[7] V. Imbriani, U. Bonavolontà, G. D. Gironimo, S. E. Shawish, et al., Insulated fixation system of plasma facing components to the divertor cassette in Eurofusion-DEMO, Fusion Eng. Des. 158 (2020) 111710, doi:10.1016/j.fusengdes.2020.111710

[8] D. Marzullo, G. D. Gironimo, U. Bonavolontà, V. Imbriani, CAD Design – 2nd phase – 2019, EFDA Report, EFDA D 2NL4LT (2019).

[9] S. El Shawish, L. Giannone, Shunt analysis in the isolated-target divertor model for plasma detachment measurement in DEMO, Fusion Eng. Des. 161 (2020) 112058, doi:10.1016/j.fusengdes.2020.112058

[10] J. You, E. Visca, C. Bachmann, et al., European DEMO divertor target: operational requirements and material-design interface, J. Nucl. Mater. 9 (2016) 171, doi:10.1016/j.nme.2016.02.005

[11] P. A. D. Maio, R. Forte, R. Gaglio, J.H. You, et al., On the thermal-hydraulic performances of the DEMO divertor cassette body cooling circuit equipped with a liner, Fusion Eng. Des. 156 (2020) 111613, doi:10.1016/j.fusengdes.2020.111613

[12] C. Bachmann, W. Biel, S. Ciattaglia, et al., Initial definition of structural load conditions in DEMO, Fusion Eng. Des. 124 (2017) 633, doi:/10.1016/j.fusengdes.2017.02.061

[13] C. Bachmann, DEMO Plant Structural Load Specification, Version 1.3, EFDA D 2MY7H3 (2019).

[14] S. El Shawish, L. Giannone, Initial CAD studies and engineering analysis, including diagnostic integration on DEMO, EFDA Report, EFDA-2P89BX (2020).

[15] A. Werner, M. Endler, J. Geiger, R. Koenig, W7-X magnetic diagnostics: Rogowski coil performance for very long pulses, Rev. Sci. Instrum. 79 (2008) 10F122, doi:10.1063/1.2957933

[16] A. Quercia, R. Albanese, R. Fresa, et al., Performance analysis of Rogowski coils and the measurement of the total toroidal current in the ITER machine, Nucl. Fusion 57 (2017) 126049, doi:10.1088/1741-4326/aa86fd

[17] T. Nishitani, G. Vayakis, M. Yamauchi, et al., Radiation-induced thermoelectric

sensitivity in the mineral-insulated cable of magnetic diagnostic coils for ITER, J. Nucl. Mater. 329 (2004) 1461, doi:10.1016/j.jnucmat.2004.04.252

[18] G. Mazzone, J. Aktaa, C. Bachmann, et al., Choice of a low operating temperature for the DEMO EUROFER97 divertor cassette, Fusion Eng. Des. 124 (2017) 217, doi:10.1016/j.fusengdes.2017.02.013

[19] P. Frosi, C. Bachmann, G. D. Gironimo, et al., Structural analysis of DEMO divertor cassette body and design study based on RCC-MRx, Fusion Eng. Des. 124 (2017) 628, doi:10.1016/j.fusengdes.2017.02.062

[20] P. Frosi, P. A. Di Maio, D. Marzullo, et al., Further improvements in the structural analysis of DEMO divertor cassette body and design assessment according to RCC-MRx, Fusion Eng. Des. 138 (2019) 119, doi:10.1016/j.fusengdes.2018.11.008

[21] G. Pautasso, L. Giannone, O. Gruber, et al., The halo current in ASDEX Upgrade, Nucl. Fusion 51 (2011) 043010, doi:10.1088/0029-5515/51/4/043010

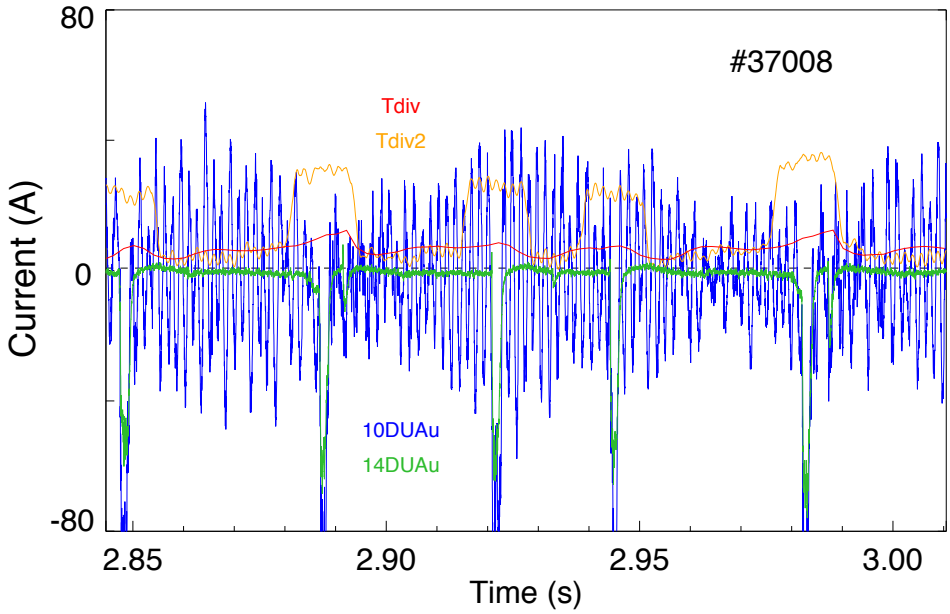

Figure 11: *Viewing shunt currents with higher time resolution, one observes that oscillations in the 50 μΩ (10DUAu) measurement dominate the ELM spikes seen clearly in the current by the 2 mΩ (14DUAu) shunt measurement.*

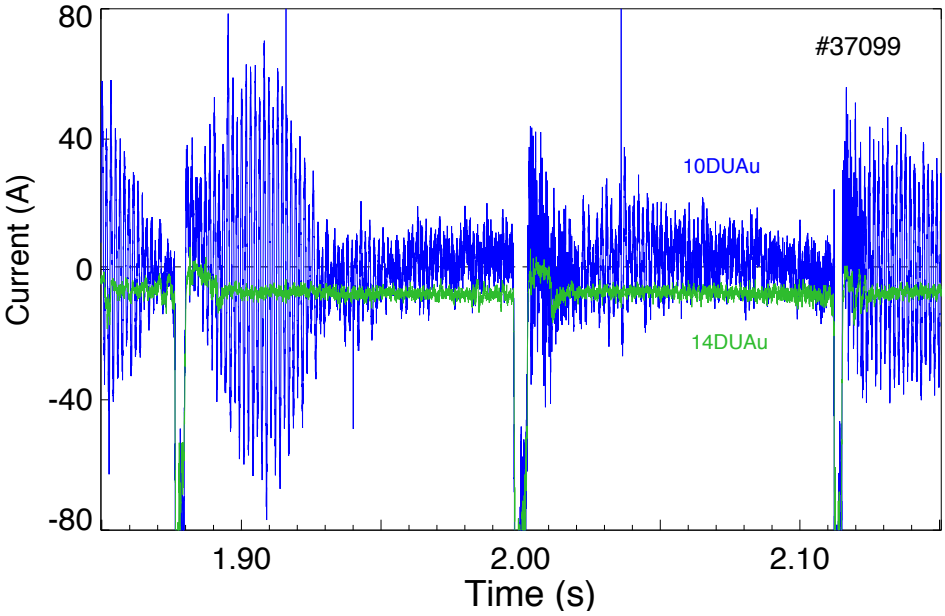

Figure 12: *Viewing shunt currents with higher time resolution in a discharge with lower ELM frequency, one observes that oscillations in the 50 $\mu\Omega$ (10DUAu) shunt measurement vary in frequency and dominate the ELM spikes.*